Ubiquitination regulates the assembly of VLDL in HepG2 cells and is the committing step of the apoB-100 ERAD pathway[S]

Eric A. Fisher, Neeraj A. Khanna, and Roger S. McLeod[1]

Department of Biochemistry & Molecular Biology, Dalhousie University, Halifax, Nova Scotia, Canada B3H 1X5

Abstract **Apolipoprotein B-100 (apoB-100) is degraded by endoplasmic reticulum-associated degradation (ERAD) when lipid availability limits assembly of VLDLs. The ubiquitin ligase gp78 and the AAA-ATPase p97 have been implicated in the proteasomal degradation of apoB-100. To study the relationship between ERAD and VLDL assembly, we used small interfering RNA (siRNA) to reduce gp78 expression in HepG2 cells. Reduction of gp78 decreased apoB-100 ubiquitination and cytosolic apoB-ubiquitin conjugates. Radiolabeling studies revealed that gp78 knockdown increased secretion of newly synthesized apoB-100 and, unexpectedly, enhanced VLDL assembly, as the shift in apoB-100 density in gp78-reduced cells was accompanied by increased triacylglycerol (TG) secretion. To explore the mechanisms by which gp78 reduction might enhance VLDL assembly, we compared the effects of gp78 knockdown with those of U0126, a mitogen-activated protein kinase/ERK kinase1/2 inhibitor that enhances apoB-100 secretion in HepG2 cells. U0126 treatment increased secretion of both apoB100 and TG and decreased the ubiquitination and cellular accumulation of apoB-100. Furthermore, p97 knockdown caused apoB-100 to accumulate in the cell, but if gp78 was concomitantly reduced or assembly was enhanced by U0126 treatment, cellular apoB-100 returned toward baseline. This indicates that ubiquitination commits apoB-100 to p97-mediated retrotranslocation during ERAD.** **Thus, decreasing ubiquitination of apoB-100 enhances VLDL assembly, whereas improving apoB-100 lipidation decreases its ubiquitination, suggesting that ubiquitination has a regulatory role in VLDL assembly.**—Fisher, E. A., N. A. Khanna, and R. S. McLeod. **Ubiquitination regulates the assembly of VLDL in HepG2 cells and is the committing step of the apoB-100 ERAD pathway.** ***J. Lipid Res.*** **2011.** 52: **1170–1180.**

Supplementary key words endoplasmic reticulum-associated degradation • apolipoprotein B-100 • very low density lipoprotein

Apolipoprotein (apo) B-100 is the major protein component of VLDLs. Assembly of VLDL in the liver begins at the endoplasmic reticulum (ER) with the formation of a primordial lipoprotein. As apoB-100 enters the ER lumen cotranslationally, it must associate with sufficient lipids for VLDL assembly to proceed. The microsomal triglyceride transfer protein (MTP) facilitates transfer of lipids onto nascent apoB-100 (1). ApoB-100 is somewhat unique in that its secretion can be regulated by degradation (2), whereas control of expression of most proteins is at the level of mRNA transcription or translation. During conditions that limit lipid supply, such as low MTP activity (3) or reduced lipid availability (4, 5), apoB-100 is delivered to and degraded by the cytosolic proteasome in a process termed ER-associated degradation (ERAD). ApoB-100 contains large hydrophobic regions that require lipidation during apoB-100 synthesis or the nascent protein is targeted to ERAD (6). In a process that remains poorly defined, apoB-100 can be secreted only if lipidation/assembly satisfies the quality control surveillance system in the secretory pathway.

The ERAD pathway removes malfolded proteins from the ER lumen or membrane [reviewed in (7)]. ERAD helps reduce the burden on ER-resident chaperones and allows the cell to maintain ER homeostasis. The typical ERAD pathway for a protein in the secretory pathway consists of at least the following steps: substrate recognition, retrotranslocation from the ER into the cytosol and ubiquitination, followed by degradation in the proteasome.

This work was presented at the Arteriosclerosis, Thrombosis, and Vascular Biology Conference, San Francisco, CA (April 8–10, 2010) and was supported by the Canadian Institute of Health Research (CIHR, MOP-89379). E.A.F. is supported by a Student Research Salary Award from the Nova Scotia Health Research Foundation.

Manuscript received 29 September 2010 and in revised form 17 March 2011.

Published, JLR Papers in Press, March 18, 2011
DOI 10.1194/jlr.M011726

Abbreviations: apo, apolipoprotein; BiP, binding immunoglobulin protein; ER, endoplasmic reticulum; ERAD, endoplasmic reticulum-associated degradation; ERK, extracellular-signal-regulated kinase; gp78, E3 ubiquitin ligase glycoprotein 78; Hsp, heat shock protein; MEK, mitogen-activated protein kinase kinase/ERK kinase; MTP, microsomal triglyceride transfer protein; NT, nontargeting; OA, oleic acid; RIPA, radioimmunoprecipitation assay; siRNA, small interfering RNA; TG, triacylglycerol; UPR, unfolded protein response; VCP, valosin-containing protein.

[1]To whom correspondence should be addressed.
e-mail: rmcleod2@dal.ca

[S] The online version of this article (available at http://www.jlr.org) contains supplementary data in the form of Materials and Methods and four figures.

These steps require cooperation between luminal chaperones, integral membrane proteins, cytosolic chaperones, and the proteasome. Some of these ERAD components have been implicated in the proteasomal degradation of apoB-100 (8).

During apoB-100 biogenesis, competition between lipidation and the degradative machinery may govern the level of VLDL secretion (9). When lipidation is insufficient to support VLDL assembly, the cotranslational entry of apoB into the ER lumen through the Sec61 translocon is delayed, causing portions of the newly synthesized apoB to become cytosolically exposed (10). This 'translocation arrest' gives nascent apoB-100 a bitopic topology, defined as simultaneous exposure to the cytosol and ER lumen. It is possible that this unique conformation initiates the ERAD of apoB-100 but it is unclear what factor(s) are necessary and sufficient for substrate recognition. On one hand, poor apoB lipidation could create exposed hydrophobic domains in the ER lumen that attract specific chaperones, whereas on the other hand, cytosolic exposure of newly translated apoB-100 epitopes may provoke interaction with cytosolic components of the ERAD machinery. Furthermore, delayed movement through the translocon may contribute to activation of ERAD as well.

The ER chaperone glucose-regulated protein 78/binding immunoglobulin protein (Grp78/BiP) associates with nascent apoB-100 when the interaction between MTP and apoB-100 is disrupted (11). Prolonged association with BiP may initiate removal of a poorly folded apoB polypeptide. It has been shown by us (12) and by Rutledge et al. (11) that the ATPase associated with various cellular activities (AAA-ATPase) p97 (also called valosin-containing protein, VCP) is involved in the removal of apoB-100 from the ER into the cytosol and facilitates its proteasomal degradation. Members of the cytosolic heat shock protein (Hsp) family, including Hsp70 and Hsp90 (13, 14), also have roles in apoB-100 degradation. These chaperones may maintain cytosolic polypeptides in an unfolded state that is suitable for efficient proteasomal degradation. Overexpression of the E3 ubiquitin ligase glycoprotein 78 (gp78) (also known as autocrine motility factor receptor) in HepG2 cells increased apoB-100 ubiquitination and degradation while decreasing apoB-100 secretion (15). To date, this is the only ubiquitin ligase implicated in the ERAD pathway of apoB-100. Gp78 can interact directly with p97 via a VCP-interaction motif to form a complex that coordinates retrotranslocation and ubiquitination of substrates from the ER for degradation (16). This led us to speculate about the functional relationship between gp78 and p97 in apoB-100 ERAD.

In the HepG2 cell line, apoB-100 secretion is limited by inefficient mobilization of lipids to the site of VLDL assembly. As a result, the majority of apoB-100-containing lipoprotein secreted from HepG2 cells is in the LDL density, rather than the mature VLDL secreted by primary hepatocytes. Furthermore, a large portion of nascent apoB-100 is removed from the secretory pathway and degraded by ERAD. Recently, it was reported that the VLDL assembly "defect" in HepG2 cells could be corrected by inhibiting MEK/ERK signaling using the compound U0126 (17). The exact mechanism is unclear. In this study, we examined the relationship between enhanced VLDL assembly, p97-mediated retrotranslocation, and gp78-dependent ubiquitination on the stability and secretion of apoB-100 in HepG2 cells.

MATERIALS AND METHODS

Cell culture

HepG2 cells were obtained from the American Type Culture Collection (ATCC, Manassis, VA; HB-8065). Cells were maintained in 10 cm culture dishes (Falcon) in DMEM (Invitrogen Corp., Burlington, ON) supplemented with 2 mM glutamine. Cells were split by trypsinization at ~70–80% confluence every two days. For experiments, cells were either plated onto 35 mm Primaria dishes or 12-well tissue culture plates [for small interfering (si)RNA transfection]. Unless indicated otherwise, cells were maintained in a 37°C humidified incubator with 5% CO_2 atmosphere. Where indicated, 70–80% confluent monolayers were treated with 25 μM MG132 (BIOMOL International, Plymouth Meeting, PA) or with 1 or 10 μM U0126 (Promega, Madison, WI).

Immunoblotting

Proteins were resolved by SDS-PAGE, transferred to nitrocellulose membranes, and visualized by immunoblotting with antibodies to apoB (1D1; Ottawa Heart Institute Research Corp., Ottawa, ON), ubiquitin (SPA-203: Stressgen Bioreagents, Ann Arbor, MI), calnexin (SPA-865; Stressgen), p97 (PRO65278; Research Diagnostics Inc., Concord, MA), heat shock protein 70 (SPA-820; Stressgen), BiP/ Glucose-regulated protein 78 (GL-19, Sigma-Aldrich), and actin (MAB1501, Chemicon, Temecula, CA). Secondary antibodies were mouse- or rabbit-specific HRP conjugates purchased from Chemicon. All immunoblots were developed using BM chemiluminescence (POD) from Roche Diagnostics.

Reduction of HepG2 p97 and gp78 with siRNA

For each well of a 12-well plate, transfection medium was prepared containing either nontargeting siRNA #1 (Dharmacon, Inc.), p97/VCP siRNA (si-p97, ID:119276, Ambion, Inc., Austin, TX), or one of two different gp78-targeting duplexes (si-gp78, ID:9537, Ambion or si-gp78-A, HSS100448, Invitrogen) and siPORT NeoFX transfection reagent (Ambion) adjusted to a final volume of 100 μl using Opti-MEM I medium (Invitrogen). HepG2 cells, at 70–80% confluence, were trypsinized and resuspended in low serum growth medium (2% FBS in DMEM). Suspended cells were added to the 100 μl transfection medium in each well to a final volume of 1 ml and siRNA concentration of 50 nM. The transfection medium was replaced with growth medium 24 h after transfection and subsequent analyses were performed 72 h following transfection. The efficiency of the siRNA knockdown was determined by immunoblotting of cell lysates for p97 protein and by quantitative polymerase chain reaction for the gp78 mRNA levels (see below).

Quantitative PCR

RNA was isolated from HepG2 cells with the RNeasy Plus Mini Kit (#74134; Qiagen). Reverse transcription for each RNA was performed as follows: 2 μg RNA and 0.2 mM of each deoxynucelotide triphosphate (dNTP) and 500 ng Oligo dT were brought to 12 μl with water and heated for 5 min at 65°C and then cooled to 4°C for 5 min. Added to this mixture were 10 mM DTT, 5× 1st strand buffer, and 200 U Superscript II enzyme (18064-014, Invitrogen) for a final volume of 20 μl per tube. Samples were incubated at 42°C for 50 min, 94°C for 15 min, and

cooled to 4°C. Each PCR reaction tube contained the following: 4 μl of the reverse transcriptase reaction, 10 μl Platinum SYBR Green Supermix-UDG (11733, Invitrogen), 250–300 nM of each the forward and reverse primers, and was brought to 20 μl total volume with water. Reactions were heated at 50°C for 2 min, 95°C for 2 min, and then subjected to 40 cycles of: 95°C 15 s, 65°C 30 s, 72°C 30 s. Knockdown efficiency (%) was determined by comparing the ΔCt values between treatments, normalized to cyclophilin as a housekeeping gene.

Metabolic labeling

HepG2 cells in 35 mm Primaria dishes at ~70–80% confluence were incubated in cysteine/methionine-free DMEM for 1 h and then incubated for 1 to 3 h, depending on the experiment, in cysteine/methionine-free DMEM containing 100 μCi of [^{35}S]cysteine/methionine (Express Protein Labeling Mix, Perkin-Elmer, Boston, MA). Where indicated, cells were supplemented with 360 μM oleic acid (OA) or 10% BSA (vehicle only) during the depletion, pulse, and chase periods. U0126 or MG132 treatments (or DMSO only) where carried through all incubations. For analysis of steady-state apoB-100 synthesis and secretion, the labeling medium was removed after 3 h and the cells were recovered by lysis as described below. For pulse-chase analysis of apoB stability and secretion, the labeling medium was removed after a 1 h pulse and the monolayers were incubated with DMEM containing 2 mM methionine and 0.6 mM cysteine plus any indicated supplements. Cells and medium were collected by lysis in a radioimmunoprecipitation assay (RIPA) buffer (50 mM Tris-HCl pH 8.0, 150 mM NaCl, 1 mM EDTA, 1% Triton X-100) containing 1% SDS as previously described (6).

Immunoprecipitation

Cell and medium samples were diluted to 0.1% SDS and apoB protein was collected by immunoprecipitation with a goat polyclonal antibody to human apoB (AB742; Chemicon). Immunocomplexes were recovered on protein A Sepharose beads (Amersham Biosciences, Inc., Baie d'Urfé, QC), washed and eluted into SDS-PAGE sample buffer. ApoB-100 was resolved by 5% SDS-PAGE and visualized by autoradiography. Radioactivity was quantified from excised gel bands by liquid scintillation counting. A polyclonal antibody to human apoAI (Roche Diagnostics, Laval, QC) was used to immunoprecipitate HepG2 apoAI. Immune complexes were resolved by SDS-PAGE on 10% (w/v) polyacrylamide gels.

Digitonin permeabilization of HepG2 cells

Confluent monolayers of HepG2 cells were incubated in CSK buffer (10 mM PIPES pH 6.8, 0.3 M sucrose, 0.1 M KCl, 2.5 mM $MgCl_2$, 1 mM sodium-free EDTA) with or without digitonin (75 μg/ml) for 10 min on ice (18). Cytosol fractions were collected and membrane fractions were recovered by lysis in 1% SDS as described above.

Ubiquitination analysis

HepG2 cells were incubated in the absence or presence of 25 μM MG132 for the indicated time. Where indicated, cells were then permeabilized with digitonin and cytosol and membrane fractions were collected. Lysates were adjusted to 0.1% SDS and apoB was collected by immunoprecipitation with polyclonal antibody to human apoB and protein A Sepharose as described above. After several washes in RIPA buffer containing 0.1% SDS, the immunoprecipitant apoB was resolved by SDS-PAGE (5%), transferred to nitrocellulose, and immunoblotted with monoclonal antibodies to apoB (1D1) or ubiquitin.

Sucrose density gradient ultracentrifugation

Medium was collected from radiolabeled HepG2 cells, brought to 12.5% sucrose, and a discontinuous sucrose gradient was prepared as described previously (19). After ultracentrifugation for 20 h at 55,000 rpm in a SW60Ti rotor, 12 fractions of 330 μl were collected. Immunoprecipitation, SDS-PAGE, and quantification of labeled apoB-100 were performed as described above.

Metabolic labeling of glycerolipids

HepG2 cells were pretreated (16 h) with 10 μM U0126 or were transfected with siRNA 72 prior to labeling. Cells were labeled for 2 h with 10 μCi/ml [2-^{3}H] glycerol (3.00 Ci/mmol; Amersham GE Healthcare) and incubated with 360 μM OA and/or 10 μM U0126 where indicated. Medium samples were collected and cell monolayers were harvested in PBS. Lipid extraction was performed using chloroform-methanol (2:1, by volume) and lipids were separated by TLC on Silica Gel 60 precoated plates for TLC (20 × 20 cm, 250 μm thickness) using L-α-phosphatidylcholine, cholesterol oleate, and triolein as lipid standards (20). Plates were visualized with iodine, TG and L-α-phosphatidylcholine bands were collected, and radioactivity was quantified by liquid scintillation counting.

Trypsin digestion in permeabilized cells

Transfected HepG2 cells were permeabilized with digitonin (described above), and washed to remove cytosol contents. Permeabilized cells were placed on ice and incubated for 30 min with the indicated concentration of trypsin (Boehringer Mannheim, QC) in CSK buffer. Soybean trypsin inhibitor (Boehringer Mannheim) was then added to a final concentration of 500 μg/ml. Cell lysis and immunoblot analysis of apoB-100 and calnexin were performed as described above.

RESULTS

Gp78 siRNA reduces apoB-100 ubiquitination and cotranslational accumulation during proteasome inhibition

To examine the functional relationship between gp78 and apoB-100 metabolism, we used an RNA interference strategy to reduce gp78 expression in HepG2 cells. It has been previously reported that overexpression of gp78 in HepG2 cells enhances apoB-100 ubiquitination and decreases apoB-100 secretion (15). Cells transfected with either a nontargeting (NT) control siRNA duplex or gp78-targeting siRNA (si-gp78) were harvested 72 h posttransfection for mRNA and protein analysis. To establish the efficiency of the si-gp78 knockdown, total RNA was isolated from the cells for real-time PCR analysis. Gp78 mRNA in the cells was reduced by 54 ± 13% (n = 3) compared with NT when normalized to cyclophilin mRNA (**Fig. 1A**). Immunoblot analysis revealed similar reductions of gp78 protein mass (data not shown).

Because gp78 is an ERAD-associated protein, reducing its expression might compromise normal protein turnover in the ER. If this were the case, ER stress caused by impaired protein turnover might trigger an unfolded protein response (UPR), the hallmark of which is increased BiP expression (21). BiP mass was not changed by the gp78 knockdown (Fig. 1B), suggesting that ER function was not compromised. Additionally, the cytosolic stress marker Hsp70 was not changed, indicating that no cytosolic heat shock response (22) was provoked by the gp78 knockdown nor was p97 expression altered (Fig. 1B). Notably, the knockdown of

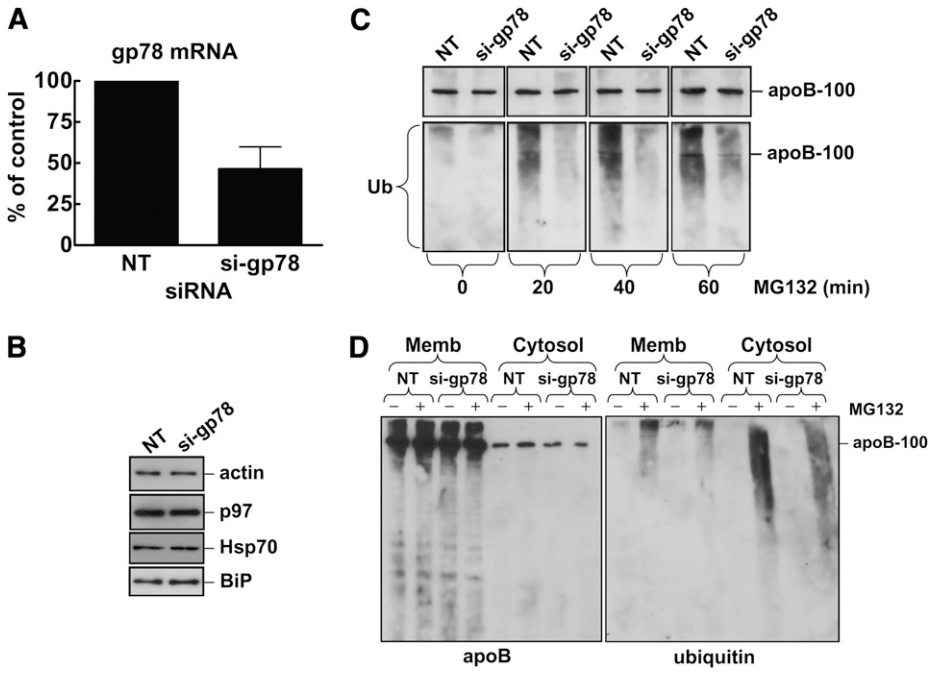

Fig. 1. siRNA-mediated reduction of gp78 decreases the accumulation of ubiquitinated apoB-100. HepG2 cells were transfected with nontargeting (NT) or gp78-targeting siRNA (si-gp78). A: Quantitative PCR analysis of gp78 mRNA at 72 h posttransfection, normalized to cyclophilin mRNA. Mean ± SD, n = 3. B: Seventy-two hours posttransfection total cell lysates were collected, resolved by SDS-PAGE, and transferred to nitrocellulose. Cellular proteins in NT and si-gp78 cells were detected by immunoblot analysis. C: Seventy-two hours posttransfection, cells were treated with 25 μM of the proteasome inhibitor MG132 for up to 1 h. ApoB-100 was immunoprecipitated from cell lysates and apoB-100 and ubiquitin were detected by immunoblot analysis. D: Cells were transfected and then treated for 30 min with or without 25 μM MG132. Cells were then permeabilized with digitonin and separated into the membrane (Memb) and cytosol (Cytosol) fractions. ApoB was recovered by immunoprecipitation and apoB (left panel) and ubiquitin (right panel) revealed by immunoblotting.

gp78 did not alter the level of apoB-100 in HepG2 cells as detected by immunoblot (Fig. 1C, top panels).

To examine the role of gp78 in apoB degradation, cells transfected with NT or gp78 siRNA were treated with the proteasome inhibitor MG132 for up to one h. Cells transfected with NT siRNA accumulated ubiquitinated apoB polypeptides (Fig. 1C, lower panels), visible in the apoB immunoprecipitates as a characteristic smear detected with an anti-ubiquitin antibody. In contrast, the cells transfected with gp78 siRNA accumulated far less ubiquitinated apoB protein, suggesting that gp78 expression is responsible for the generation of apoB-ubiquitin conjugates. These data complement previous observations (15) where gp78 overexpression increased the ubiquitination of apoB in HepG2 cells.

Digitonin permeabilization was used to examine cytosolic apoB with or without gp78 knockdown. As indicated in the left panel of Fig. 1D, the majority of apoB was found in the membrane fraction (Memb, deliberately overexposed to reveal the cytosolic apoB). Upon treatment of NT cells with MG132, apoB-ubiquitin conjugates accumulated in both the membrane and cytosol fractions (right panel), with the lower molecular weight poly-ubiquitinated species found only in the cytosol fraction. In contrast to NT-transfected cells, the gp78-reduced cells contained less apoB-ubiquitin conjugates in the cytosol and fewer ubiquitin-positive apoB-100 proteins in the membrane fraction (Fig. 1D). This suggested that gp78 mediates efficient ubiquitination and contributes to the production of lower molecular weight apoB-ubiquitin conjugates in the cytosol.

In MG132 treated cells, the lower molecular weight apoB-ubiquitin pool detected by immunoblotting could be generated cotranslationally (ubiquitinated, incompletely translated apoB-100 protein). To explore this, we monitored apoB-100 synthesis using metabolic labeling (0–20 min) of puromycin synchronized cells (supplementary Fig. I). Inclusion of MG132 caused the accumulation of incomplete apoB polypeptides in NT cells (left panel, +MG132 compared with –MG132 at 5, 10, 20 min). In contrast, in gp78-reduced cells, the pattern of incomplete apoB polypeptides was not markedly different with or without MG132 (right panel). This suggested that efficient cotranslational targeting of apoB to ERAD requires gp78 expression.

Gp78 knockdown increases apoB and triglyceride secretion and shifts the secreted apoB-100 particle density to VLDL from LDL

To examine the effect of reduced gp78 expression on newly synthesized apoB-100, we monitored intracellular turnover and secretion using pulse-chase radiolabeling.

Cells were pulse-labeled for 1 h with [^{35}S]cysteine/methionine, and cells and media were then collected after a 2 h chase and analyzed for levels of radiolabeled apoB-100 and apoAI. In the gp78-reduced cells, apoB-100 secretion was increased by nearly 30% (**Fig. 2A**) over the NT-transfected cells but apoB-100 stability was not increased by gp78 knockdown. Secretion of apoAI was not impaired by the gp78-knockdown (Fig. 2B), indicating that the secretory pathway was not compromised.

We hypothesized that the increase in apoB-100 secretion might reflect the production of small, dense, poorly lipidated lipoproteins that had escaped degradation. To examine the effect of gp78 knockdown on VLDL assembly, chase medium was fractionated by density gradient ultracentrifugation and radiolabeled apoB-100 was recovered from each fraction. Unexpectedly, we observed a shift in the secretion profile in gp78 knockdown cells compared with NT control cells (**Fig. 3A**). Reduced gp78 expression increased the apoB-100 radiolabel in VLDL-sized particles (Fig. 3B). The unexpected shift in lipoprotein density was also observed with a second siRNA duplex targeting gp78 (Fig. 3A, B, si-gp78-A), demonstrating that the enhanced VLDL assembly was not an off-target effect of that particular siRNA.

It appeared that when gp78 expression was reduced, the apoB protein could acquire more lipid than NT control cells, because the decreased density of the secreted lipoproteins is indicative of an increased lipid-to-protein ratio. [^{3}H]Glycerol labeling revealed that triglyceride secretion was modestly increased by the gp78 knockdown in the presence of oleic acid (Fig. 3C). Interestingly, triglyceride synthesis from glycerol was reduced in si-gp78 cells (Fig. 3D) but this did not compromise TG secretion. Notably, gp78 reduction did not alter the levels of several proteins involved in lipid metabolism including diacylglycerol acyltransferase-1 (DGAT1), MTP, HMG-CoA reductase, sterol regulatory element-binding protein 1a (SREBP1a), peroxisome proliferator-activated receptor (PPAR)-α and PPARγ. (supplementary Fig. II).

Reduction of gp78 alters the cytosolic exposure of apoB-100

It has been shown that a portion of the cellular apoB-100 pool is cytosolically exposed as it progresses through the secretory pathway (23, 24). The extent of cytosolic exposure of apoB-100 could affect its susceptibility to degradation. We hypothesized that reduced ubiquitination might decrease the cytosolic exposure of apoB-100. To test this, permeabilized NT and si-gp78 cells were trypsin digested to destroy proteins not protected within the microsomal and nuclear membrane compartments. The ER-luminal N-terminus of calnexin was protected against trypsin digestion in both NT and si-gp78 cells (**Fig. 4A**). ApoB-100 was sensitive to trypsin digestion but more apoB-100 was protected in si-gp78 than in NT cells (Fig. 4B). A radiolabeling approach also revealed improved protection of apoB-100 against trypsin digestion with si-gp78 when normalized to apoA-I (supplementary Fig. III). This suggested that reduced gp78 expression alters the membrane topology of apoB-100.

Inhibition of ERK1/2 phosphorylation in HepG2 cells improves VLDL assembly, lipid incorporation, and secretion

As previously reported (17), we found that the MEK inhibitor U0126 shifted the apoB-100 density profile in a dose-responsive manner from LDL to VLDL when radiolabeled cell culture medium was examined by gradient ultracentrifugation (**Fig. 5A**, B).

To examine the secretion of cellular TG, U0126-treated cells were incubated with [2-^{3}H]glycerol for 2 h, followed by collection and analysis of [^{3}H]TG from the cells and media. U0126 did not stimulate incorporation of [^{3}H]glycerol into cellular TG, whereas oleic acid induced a large increase in cellular [^{3}H]TG levels (Fig. 5C). Secretion of [^{3}H]TG into the medium was modestly stimulated by either U0126 or OA, and there was a more than additive effect on [^{3}H]TG secretion when U0126 and oleic acid were added together (Fig. 5D). Taken together, these observations

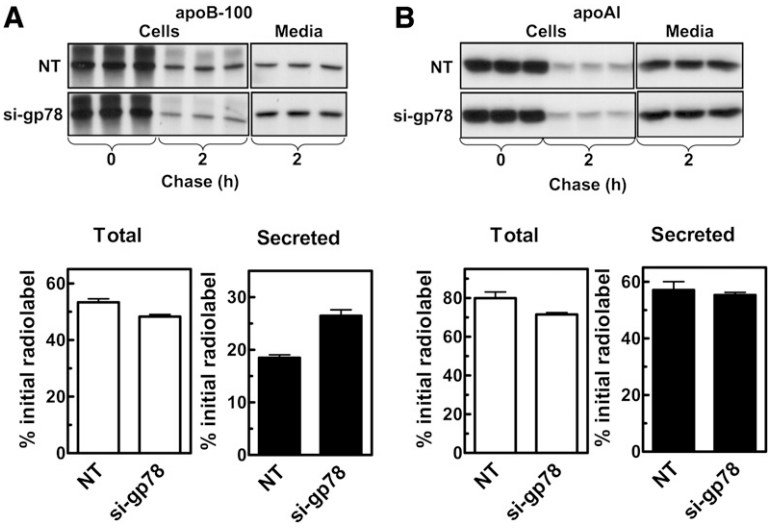

Fig. 2. siRNA-mediated reduction of gp78 increases apoB-100 secretion. Autoradiographs and quantitation of apoB-100 (A) and apoAI (B) in cells and medium by pulse-chase analysis. Seventy-two hours following transfection with either nontargeting (NT) or gp78-targeting (si-gp78) siRNA, HepG2 cells were labeled with [^{35}S]cysteine/methionine for 1 h and then chased for 2 h as described in Materials and Methods. ApoB and apoAI were recovered from cells and media by immunoprecipitation and visualized in SDS-PAGE gels by autoradiography (top panels). Total (medium plus cells) and secreted radiolabeled proteins are expressed as percent of initial radiolabel. Autoradiographs and quantitation (mean ± SD) are derived from triplicate wells from a representative experiment, which was repeated three times.

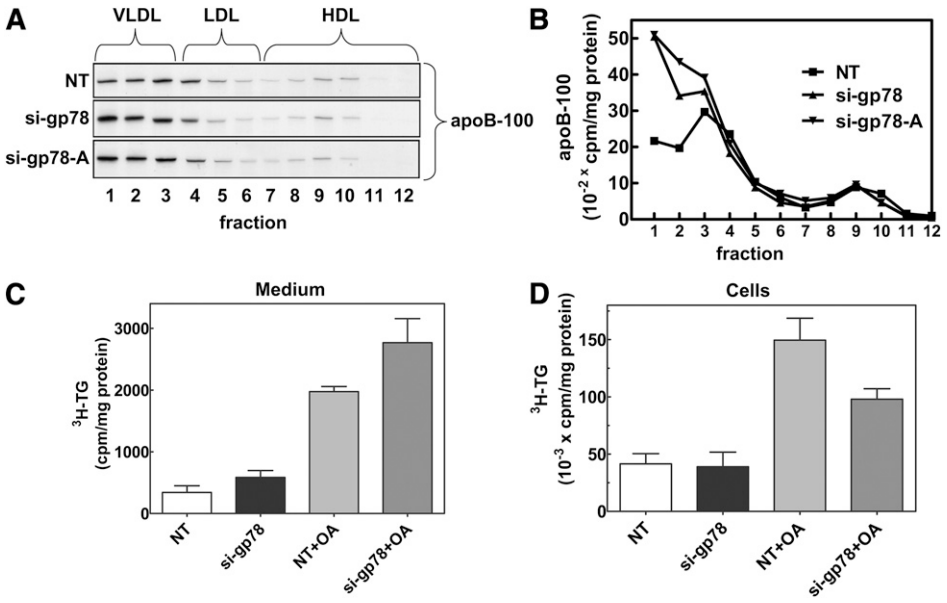

Fig. 3. siRNA-mediated reduction of cellular gp78 enhances VLDL and triglyceride secretion from HepG2 cells. A: Density gradient ultracentrifugation profiles of secreted apoB-100. Cells were transfected with either NT siRNA or siRNA duplexes targeting gp78 (si-gp78 or si-gp78-A). Seventy-two hours posttransfection, cells were depleted for 1 h in cysteine/methionine-free media and then pulse-labeled for 1 h with [^{35}S]cysteine/methionine. Pulse medium was replaced with chase medium for 2 h after which medium samples were collected. Samples were subjected to density gradient ultracentrifugation and apoB was immunoprecipitated from each fraction and visualized by SDS-PAGE and autoradiography. B: Quantitation of apoB-100. Radiolabeled apoB-100 bands were excised from the gel and quantified by liquid scintillation counting. Results are expressed as cpm per mg cell protein. The data presented is representative of three experiments. C, D: Transfected HepG2 cells were labeled for 2 h with [2-^{3}H] glycerol in the presence or absence of 360 μM oleic acid. Lipids were extracted from cells and media in methanol-chloroform and separated by TLC. The triglyceride bands were visualized by iodine staining and quantified by liquid scintillation counting. Data are mean ± SD, n = 3.

suggested that the increase in cellular [^{3}H]TG with oleic acid alone did not increase [^{3}H]TG secretion markedly, but the inclusion of U0126 improved the incorporation of [^{3}H]TG into VLDL.

MEK1/2 inhibition decreases apoB-100 ubiquitination and diverts apoB-100 ERAD substrates into the secretory pathway

Based on the similar enhancement of VLDL formation in gp78 knockdown cells and with U0126 treatment, we hypothesized that apoB-100 could escape ubiquitination and degradation in U0126-treated cells because the malfolding that triggers ERAD was reduced. When MG132 and U0126 were included together, less nascent apoB accumulated than with MG132 alone (**Fig. 6A**, left panel), suggesting that U0126 reduced apoB-100 ERAD substrates. Total apoB-100 secretion was profoundly increased by U0126 but MG132 had no effect on apoB-100 secretion (Fig. 6A, right panel). As shown in Fig. 6B, U0126 and MG132, alone or together, stabilized apoB-100 during a 1 h chase compared with the untreated control. Conversely, U0126 increased apoB-100 secretion whereas MG132 did not (Fig. 6B, right panel). Because U0126 did not increase apoB-100 synthesis (Fig. 6A, left panel), the enhanced secretion appeared to represent apoB-100 that had escaped ERAD during conditions of improved lipid incorporation. Taken together, the reduced cellular apoB-100 accumulation and increased secretion suggested that MEK/ERK inhibition by U0126 reduced the entry of newly synthesized apoB into the ERAD pathway by creating an environment that favored VLDL assembly.

Immunoblot analysis (Fig. 6C) showed that U0126-treated cells accumulated much less ubiquitinated apoB following the MG132 treatments. This suggested that in these cells apoB-100 could escape from the ERAD pathway at a step before ubiquitination. The decrease in ubiquitinated apoB was not accompanied by a reduction in global ubiquitination in U0126-treated cells (supplementary Fig. IV A, left panel).

si-gp78 and U0126 treatment both reduce the apoB-100 accumulation and BiP induction observed in p97-reduced cells

The removal of apoB-100 from the ER into the cytosol for proteasomal degradation is facilitated by p97 (11, 12). Gp78 and p97 are known to associate with one another and coordinate the ubiquitination and retrotranslocation of other ERAD substrates (25). Knockdown of p97 delayed the turnover of nascent apoB-100, causing it to accumulate intracellularly (12). We hypothesized that if gp78 and p97 act in the same apoB ERAD pathway, gp78-dependent ubiquitination may occur before p97-mediated retrotranslocation and if so, gp78 knockdown in p97-reduced cells would reverse the apoB accumulation and enhance secretion.

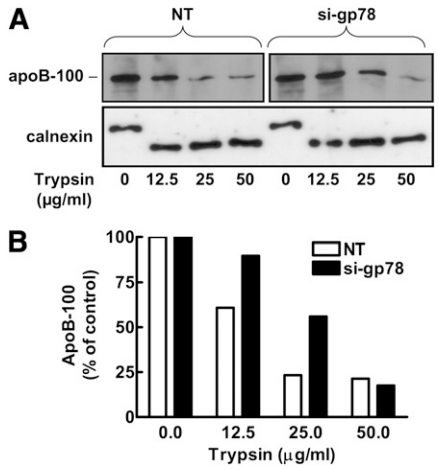

Fig. 4. Reduced gp78 expression protects apoB-100 from trypsin digestion in digitonin-permeabilized HepG2 cells. A: Cells were transfected with either nontargeting (NT) or gp78-targeting siRNA. Seventy-two hours posttransfection the cells were permeabilized with digitonin and the supernatant was discarded, leaving only the nuclear and microsomal membranes intact. The remaining monolayers were then treated with trypsin at the indicated concentration for 30 min on ice. Soybean trypsin inhibitor was added and the monolayers were collected. Calnexin and apoB were visualized in each sample by immunoblot analysis. B: ApoB-100 was quantified by scanning densitometry and is expressed as percent of 0 μg/ml trypsin control.

Furthermore, U0126 would reduce apoB accumulation in p97-reduced cells because apoB could be diverted from ERAD before ubiquitination, thus avoiding the p97-dependent step.

Transfected cells were radiolabeled for 3 h in the presence of oleic acid. Although the p97 knockdown caused marked apoB-100 accumulation relative to control cells (NT), the combined knockdown of both p97 and gp78 caused almost no accumulation of nascent apoB-100 (**Fig. 7A**, left panel). U0126 had the same effect on apoB-100 as gp78 knockdown when superimposed upon the p97 knockdown (Fig. 7B). Both gp78 knockdown and U0126 were able to enhance apoB-100 secretion from p97 knockdown cells (Fig. 7A, B, right panels). Unlike U0126, gp78 knockdown did not alter phospho-ERK1/2 levels (supplementary Fig. IV B), suggesting that the effects of gp78 reduction and U0126 treatment are mechanistically distinct.

Our previous study (12) showed an increase in BiP levels with p97 knockdown, consistent with a modest ER stress, and this was also observed here (Fig. 7C, D). Interestingly, both gp78 knockdown (Fig. 7C) and U0126 treatment (Fig. 7D) decreased the elevated BiP levels observed in p97-reduced cells. These observations suggest that either preventing ubiquitination or enhancing assembly can reduce the apoB accumulation and ER stress in p97-reduced cells.

DISCUSSION

The present work has revealed an expanded role for the ubiquitin ligase gp78 in the metabolism of apoB-100. Our knockdown experiments complement results presented in a gp78 overexpression study (15) to indicate that gp78 is a ubiquitin ligase that regulates apoB-100 ERAD. In addition, because decreasing the ubiquitination of apoB-100 can enhance VLDL assembly, it reveals a new level of complexity in the relationship between apoB secretion and ERAD. Our studies using the MEK/ERK inhibitor U0126 have shown that this compound acts by increasing the efficiency of coupling of new TG synthesis to VLDL assembly in HepG2 cells. Finally, our double knockdown experiments suggest that ubiquitination of apoB-100 in HepG2 cells occurs before the involvement of p97 and is the committing step for ERAD. Thus, poorly lipidated or translocation-arrested apoB-100 are not ERAD substrates but polyubiquitinated apoB is. These observations lend weight to the new possibility that regulation of VLDL assembly in hepatocytes may be dependent on a functional ERAD pathway.

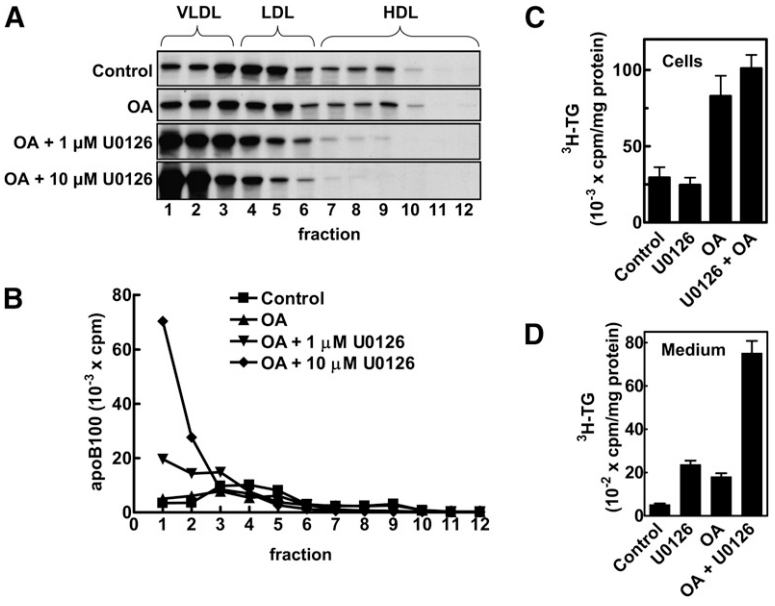

Fig. 5. U0126 treatment enhances assembly of VLDL in HepG2 cells and increases secretion of radiolabeled triglycerides. HepG2 cells were treated with 1 or 10 μM U0126 for 16 h. Cells were then incubated in the presence or absence of 360 μM oleic acid and labeled with [^{35}S]cysteine/methionine for 3.5 h. After labeling, the media were fractionated by sucrose density gradient ultracentrifugation and each fraction was subjected to apoB immunoprecipitation using goat anti-human apoB antibody. A: Eluted proteins were resolved on a 5% SDS-PAGE gel, visualized by autoradiography. B: The radioactivity in apoB-100 was quantified by scintillation counting. C, D: HepG2 cells were treated with 10 μM U0126 for 16 h were labeled for 2 h with [2-^{3}H] glycerol in the presence or absence of 360 μM oleic acid. Lipids were extracted from cells (C) and media (D) in methanol-chloroform and separated by TLC. The triglyceride bands were visualized by iodine staining and quantified by liquid scintillation counting. Values are mean ± SD, n = 3.

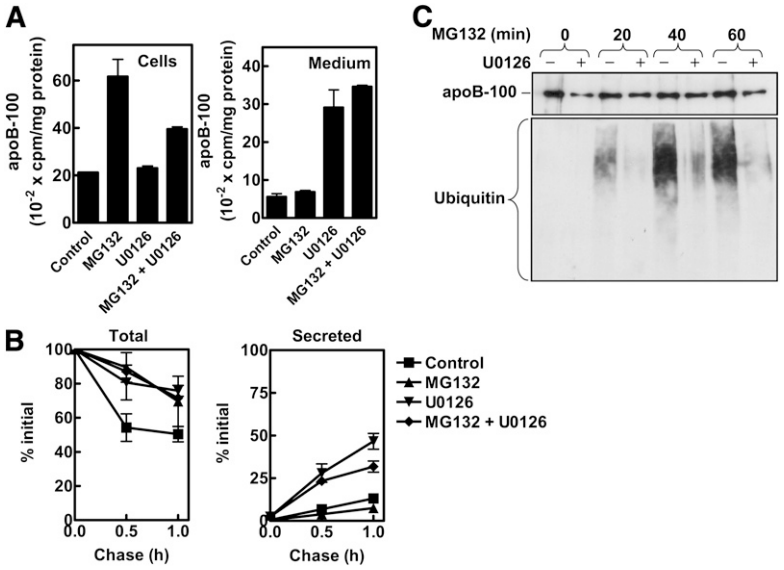

Fig. 6. U0126 treatment reduces cell apoB-100 ubiquitination and enhances secretion. A, B: HepG2 cells were treated with U0126 for 16 h. Cells were then incubated for 1 h with 360 μM oleic acid, with or without 25 μM MG132, before a 1 h pulse with [^{35}S]cysteine/methionine. Labeled apoB-100 was collected by immunoprecipitation, resolved by SDS-PAGE, and quantified by liquid scintillation counting. A: Cells and media were collected after the pulse period. Data are mean and range of duplicates. B: Medium was removed and replaced with chase medium and cells and media were collected after the indicated chase time. Data are mean ± SD, n = 3. C: U0126-treated cells (16 h) were incubated for 1 h with 360 μM oleic acid prior to MG132 treatment for the indicated time period. ApoB immunoprecipitates were collected from cell lysates and analyzed by immunoblotting for apoB (top panel) and ubiquitin (bottom panel).

Our data suggest that a portion of HepG2 apoB-100 that would normally be degraded by the ERAD pathway can continue through the secretory pathway to a different fate when ubiquitination or lipidation is modulated. Decreased ubiquitination (by gp78 knockdown) and improved lipid incorporation (by inhibiting ERK1/2 phosphorylation with U0126) both enhanced the secretion of apoB-100 and lipids without increasing cellular apoB-100 levels. U0126 did not alter global ubiquitination, and gp78 knockdown did not alter ERK1/2 phosphorylation or the expression of proteins known to regulate VLDL secretion and/or lipid metabolism (DGAT1, HMG-CoA reductase, MTP, SREBP1a, PPARα and PPARγ). To our knowledge, the only demonstrable similarity between the gp78 knockdown and U0126 are the effects on apoB-100 ubiquitination and VLDL secretion. The ERAD pathway degrades a large portion of nascent apoB and this can increase further when ubiquitination is enhanced (15). Because reduction

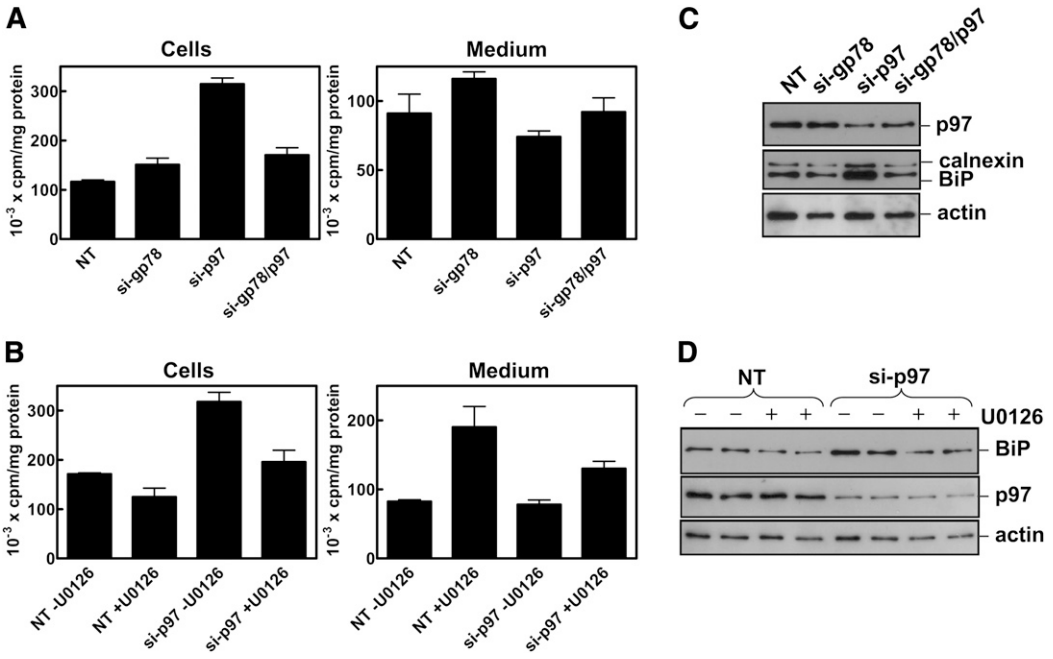

Fig. 7. Knockdown of gp78 and U0126 treatment normalize the impaired turnover of apoB-100, and BiP expression in p97 knockdown cells. A: HepG2 cells were transfected with NT, gp78, p97 siRNA, or both gp78 and p97 siRNA. Following a 1 h preincubation with 360 μM oleic acid in cysteine/methionine free media, cells were labeled with [^{35}S]cysteine/methionine in the presence of oleic acid for 3 h. Cells and media were collected and apoB-100 was recovered by immunoprecipitation, resolved by SDS-PAGE, and quantified by liquid scintillation counting. Data points represent mean ± SD (n = 3). B: Fifty-six hours posttransfection, cells with either NT or p97-targeting siRNA were treated with 10 μM U0126 for 16 h, then labeled as in A in the presence of U0126. C, D: Immunoblot analysis of cell proteins following siRNA or U0126 treatment.

of apoB ubiquitination enhances assembly, apoB substrates could be selected for ERAD based on folding/assembly kinetics during or after translation and, as a result, prevent assembly at maximum capacity. Taken together, these observations suggest that ERAD capacity and VLDL output may be linked.

In gp78 knockdown cells, newly synthesized apoB-100 was less accessible to the cytosol and secretion of both apoB-100 and TG were increased, suggesting that impaired ubiquitination influences both the topology of apoB-100 and lipid recruitment during VLDL biogenesis. If ubiquitin is ligated onto a cytosolic motif of translocation-arrested apoB-100, the branched apoB-ubiquitin conjugate could restrict translocation through the Sec61 channel. Conversely, lack of ubiquitination may allow apoB-100 to avoid prolonged exposure to the cytosol and increase the likelihood of successful translocation and VLDL assembly. The ERAD paradigm posits that recognition of malfolded protein substrates occurs prior to the involvement of ubiquitin ligase enzymes (26). U0126 treatment enhances incorporation of TG into VLDL and in so doing may allow apoB to avoid translocation arrest and escape ERAD at the substrate recognition stage. Improved lumenal lipidation and decreased cytosolic exposure (presumably due to increased translocation efficiency) occur together when apoB escapes ERAD. Nevertheless, the location and molecular nature of the recognition event(s) remain(s) unclear. ApoB-100, because of its unique exposure to the cytosol during assembly, may not require the targeting and partial retrotranslocation steps required by most ERAD substrates before their ubiquitination (7). If poorly lipidated apoB-100 is not ubiquitinated, it appears to be able to reengage with the factors that support VLDL assembly, possibly displacing ERAD substrate recognition factors.

Our data suggests a regulatory role for ubiquitination in VLDL assembly. During biogenesis, a portion of the nascent apoB-100 may exist in an intermediate, uncommitted state: not fully secretion-competent, yet not terminally malfolded. ApoB-100 contains hydrophobic β domains that bind strongly to lipids (27). Until the quality control surveillance machinery is satisfied with the status of these domains, it appears that apoB-100 must remain accountable to the ERAD pathway. ApoB-100 associates with the membrane during initial stages of assembly and then is released into the lumen during VLDL particle maturation (28, 29), coinciding with conformational changes in apoB in the Golgi (30). Cytosol-exposed apoB-100 has been observed in post-ER compartments after translation has been completed but perhaps before the final maturation step (31). Release of apoB-100 into the lumen during particle maturation may release apoB from susceptibility to proteasome-mediated ERAD. Perhaps there exist basal levels of ubiquitination that do not trigger ERAD but can be extended or removed based on temporal quality control surveillance.

When p97 is reduced, apoB-100 proteins become arrested at the ER membrane due to limited retrotranslocation (12). The accumulated apoB-100 apparently cannot reenter the assembly pathway, because oleic acid supplementation during pulse-chase radiolabeling did not elicit additional apoB-100 secretion from si-p97 cells (data not shown). However, apoB-100 can become secretion-competent if ERAD is blocked at the recognition or ubiquitination step (U0126 and gp78 knockdown, respectively). Because U0126 and gp78 knockdown normalized cellular apoB-100 turnover in si-p97 cells, our observations suggest that the gp78-dependent ubiquitination of apoB-100 is the committing step of ERAD and that p97-mediated retrotranslocation occurs thereafter.

Gp78 is an integral membrane protein that can serve as a scaffold for the assembly of protein complexes that coordinate the ERAD of several substrates (25). Gp78 can directly bind to and recruit p97 to the surface of the ER membrane (16). It is possible that decreased gp78 expression alters the stoichiometry of dedicated ERAD complexes (containing p97 and other proteins) at the ER bilayer. However, it was recently reported that the expanded polyglutamine tracts of the huntingtin protein bind the Cue domain of gp78 and sterically hinder the gp78/p97 association but do not affect the ability of gp78 to ubiquitinate the huntingtin protein (32). This suggests that the E3 ligase activity of gp78 does not depend on the formation of a p97-associated ERAD complex. Because the gp78 and p97 knockdowns have essentially opposite efects on apoB-100 fate, disrupted ubiquitination of apoB-100 is the probable cause of increased apoB-100 secretion in gp78-reduced cells.

The lack of ER stress in gp78-reduced cells may relate to the modest knockdown efficiency or may indicate that other ubiquitin ligases can partially compensate for decreased gp78 activity. The knockdown of p97 induces BiP expression to varying degrees depending on knockdown efficiency and cell type (33, 34), indicative of UPR activation (35). In our system, this stress appears to be relatively mild as it does not induce CCAAT/enhancer-binding protein homologous protein, a marker of severe, potentially apoptosis-inducing stress (data not shown), or impair the synthesis or secretion of apoB-100 or apoAI. More severe levels of UPR activation have been shown to compromise the biogenesis of apoB-100 (36). When gp78 knockdown or U0126 treatment was superimposed upon si-p97 cells, BiP levels were lower than with the p97 knockdown alone. Therefore, by modulating apoB-100 metabolism through distinct mechanisms, gp78 knockdown and U0126 are able to improve ER homeostasis in p97-reduced cells. This suggests that delayed apoB-100 turnover may be the major cause of the ER stress in p97 knockdown cells. Indeed, it was recently proposed that overproduction of the apoB-100 protein may be a "molecular link" between lipid-induced ER stress and hepatic insulin resistance (37).

Hepatic apoB-100 secretion is of emerging relevance in the regulation of plasma LDL (38). The present study highlights the importance of a functional ERAD pathway in regulating levels of apoB-100 secretion from HepG2 cells. The liver, among other organs, displays an age-related decline in protein quality control, including decreased

ability to induce expression of Hsps, including Hsp70 and Hsp90 (22, 39). With aging, compromised quality control and decreased ubiquitination could contribute to the overproduction and secretion of apoB-100. It would be interesting to examine how pathological conditions that arise in the liver affect the capacity to degrade apoB-100 by ERAD.

In conclusion, our work suggests that ubiquitination of apoB-100 has a regulatory role during VLDL assembly in HepG2 cells. Moreover, gp78 acts before and independently of p97 in the same apoB-100 ERAD pathway. Taken together, our data implicates ubiquitination as the committing step of apoB-100 to ERAD, without which the nascent protein can proceed to assemble mature VLDL.

REFERENCES

1. Shelness, G. S., and A. S. Ledford. 2005. Evolution and mechanism of apolipoprotein B-containing lipoprotein assembly. *Curr. Opin. Lipidol.* **16:** 325–332.
2. Lapierre, L. R., and R. S. McLeod. 2007. Regulation of hepatic production of lipoproteins containing apolipoprotein B by ER-associated degradation. *Future Lipidol.* **2:** 173–184.
3. Benoist, F., and T. Grand-Perret. 1997. Co-translational degradation of apolipoprotein B100 by the proteasome is prevented by microsomal triglyceride transfer protein. Synchronized translation studies on HepG2 cells treated with an inhibitor of microsomal triglyceride transfer protein. *J. Biol. Chem.* **272:** 20435–20442.
4. Dixon, J. L., S. Furukawa, and H. N. Ginsberg. 1991. Oleate stimulates secretion of apolipoprotein B-containing lipoproteins from Hep G2 cells by inhibiting early intracellular degradation of apolipoprotein B. *J. Biol. Chem.* **266:** 5080–5086.
5. Zhou, M., E. A. Fisher, and H. N. Ginsberg. 1998. Regulated cotranslational ubiquitination of apolipoprotein B100. A new paradigm for proteasomal degradation of a secretory protein. *J. Biol. Chem.* **273:** 24649–24653.
6. Lapierre, L. R., D. L. Currie, Z. Yao, J. Wang, and R. S. McLeod. 2004. Amino acid sequences within the β1 domain of human apolipoprotein B can mediate rapid intracellular degradation. *J. Lipid Res.* **45:** 366–377.
7. Vembar, S. S., and J. L. Brodsky. 2008. One step at a time: endoplasmic reticulum-associated degradation. *Nat. Rev. Mol. Cell Biol.* **9:** 944–957.
8. Rutledge, A. C., Q. Su, and K. Adeli. 2010. Apolipoprotein B100 biogenesis: a complex array of intracellular mechanisms regulating folding, stability, and lipoprotein assembly. *Biochem. Cell Biol.* **88:** 251–267.
9. Sakata, N., X. Wu, J. L. Dixon, and H. N. Ginsberg. 1993. Proteolysis and lipid-facilitated translocation are distinct but competitive processes that regulate secretion of apolipoprotein B in Hep G2 cells. *J. Biol. Chem.* **268:** 22967–22970.
10. Mitchell, D. M., M. Zhou, R. Pariyarath, H. Wang, J. D. Aitchison, H. N. Ginsberg, and E. A. Fisher. 1998. Apoprotein B100 has a prolonged interaction with the translocon during which its lipidation and translocation change from dependence on the microsomal triglyceride transfer protein to independence. *Proc. Natl. Acad. Sci. USA.* **95:** 14733–14738.
11. Rutledge, A. C., W. Qiu, R. Zhang, R. Kohen-Avramoglu, N. Nemat-Gorgani, and K. Adeli. 2009. Mechanisms targeting apolipoprotein B100 to proteasomal degradation: evidence that degradation is initiated by BiP binding at the N terminus and the formation of a p97 complex at the C terminus. *Arterioscler. Thromb. Vasc. Biol.* **29:** 579–585.
12. Fisher, E. A., L. R. Lapierre, R. D. Junkins, and R. S. McLeod. 2008. The AAA-ATPase p97 facilitates degradation of apolipoprotein B by the ubiquitin-proteasome pathway. *J. Lipid Res.* **49:** 2149–2160.
13. Zhou, M., X. Wu, L. S. Huang, and H. N. Ginsberg. 1995. Apoprotein B100, an inefficiently translocated secretory protein, is bound to the cytosolic chaperone, heat shock protein 70. *J. Biol. Chem.* **270:** 25220–25224.
14. Gusarova, V., A. J. Caplan, J. L. Brodsky, and E. A. Fisher. 2001. Apoprotein B degradation is promoted by the molecular chaperones hsp90 and hsp70. *J. Biol. Chem.* **276:** 24891–24900.
15. Liang, J. S., T. Kim, S. Fang, J. Yamaguchi, A. M. Weissman, E. A. Fisher, and H. N. Ginsberg. 2003. Overexpression of the tumor autocrine motility factor receptor Gp78, a ubiquitin protein ligase, results in increased ubiquitinylation and decreased secretion of apolipoprotein B100 in HepG2 cells. *J. Biol. Chem.* **278:** 23984–23988.
16. Zhong, X., Y. Shen, P. Ballar, A. Apostolou, R. Agami, and S. Fang. 2004. AAA ATPase p97/valosin-containing protein interacts with gp78, a ubiquitin ligase for endoplasmic reticulum-associated degradation. *J. Biol. Chem.* **279:** 45676–45684.
17. Tsai, J., W. Qiu, R. Kohen-Avramoglu, and K. Adeli. 2007. MEK-ERK inhibition corrects the defect in VLDL assembly in HepG2 cells: potential role of ERK in VLDL-ApoB-100 particle assembly. *Arterioscler. Thromb. Vasc. Biol.* **27:** 211–218.
18. Cavallo, D., R. S. McLeod, D. Rudy, A. Aiton, Z. Yao, and K. Adeli. 1998. Intracellular translocation and stability of apolipoprotein B are inversely proportional to the length of the nascent polypeptide. *J. Biol. Chem.* **273:** 33397–33405.
19. McLeod, R. S., Y. Wang, S. Wang, A. Rusinol, P. Links, and Z. Yao. 1996. Apolipoprotein B sequence requirements for hepatic very low density lipoprotein assembly. *J. Biol. Chem.* **271:** 18445–18455.
20. Wang, Y., R. S. McLeod, and Z. Yao. 1997. Normal activity of microsomal triglyceride transfer protein is required for the oleate-induced secretion of very low density lipoproteins containing apolipoprotein B from McA-RH7777 cells. *J. Biol. Chem.* **272:** 12272–12278.
21. Zhang, K., and R. J. Kaufman. 2008. From endoplasmic-reticulum stress to the inflammatory response. *Nature.* **454:** 455–462.
22. Tower, J. 2009. Hsps and aging. *Trends Endocrinol. Metab.* **20:** 216–222.
23. Borchardt, R. A., and R. A. Davis. 1987. Intrahepatic assembly of very low density lipoproteins. Rate of transport out of the endoplasmic reticulum determines rate of secretion. *J. Biol. Chem.* **262:** 16394–16402.
24. Macri, J., and K. Adeli. 1997. Conformational changes in apolipoprotein B modulate intracellular assembly and degradation of ApoB-containing lipoprotein particles in HepG2 cells. *Arterioscler. Thromb. Vasc. Biol.* **17:** 2982–2994.
25. Ballar, P., and S. Fang. 2008. Regulation of ER-associated degradation via p97/VCP-interacting motif. *Biochem. Soc. Trans.* **36:** 818–822.
26. Nakatsukasa, K., and J. L. Brodsky. 2008. The recognition and retrotranslocation of misfolded proteins from the endoplasmic reticulum. *Traffic.* **9:** 861–870.
27. Wang, L., D. D. Martin, E. Genter, J. Wang, R. S. McLeod, and D. M. Small. 2009. Surface study of apoB1694–1880, a sequence that can anchor apoB to lipoproteins and make it nonexchangeable. *J. Lipid Res.* **50:** 1340–1352.
28. Dixon, J. L., R. Chattapadhyay, T. Huima, C. M. Redman, and D. Banerjee. 1992. Biosynthesis of lipoprotein: location of nascent apoAI and apoB in the rough endoplasmic reticulum of chicken hepatocytes. *J. Cell Biol.* **117:** 1161–1169.
29. Adeli, K., M. Wettesten, L. Asp, A. Mohammadi, J. Macri, and S. O. Olofsson. 1997. Intracellular assembly and degradation of apolipoprotein B-100-containing lipoproteins in digitonin-permeabilized HEP G2 cells. *J. Biol. Chem.* **272:** 5031–5039.
30. Gusarova, V., J. Seo, M. L. Sullivan, S. C. Watkins, J. L. Brodsky, and E. A. Fisher. 2007. Golgi-associated maturation of very low density lipoproteins involves conformational changes in apolipoprotein B, but is not dependent on apolipoprotein E. *J. Biol. Chem.* **282:** 19453–19462.
31. Du, X., J. D. Stoops, J. R. Mertz, C. M. Stanley, and J. L. Dixon. 1998. Identification of two regions in apolipoprotein B100 that are exposed on the cytosolic side of the endoplasmic reticulum membrane. *J. Cell Biol.* **141:** 585–599.
32. Yang, H., C. Liu, Y. Zhong, S. Luo, M. J. Monteiro, and S. Fang. 2010. Huntingtin interacts with the cue domain of gp78 and inhibits gp78 binding to ubiquitin and p97/VCP. *PLoS ONE.* **5:** e8905.
33. Wojcik, C., M. Rowicka, A. Kudlicki, D. Nowis, E. McConnell, M. Kujawa, and G. N. DeMartino. 2006. Valosin-containing protein (p97) is a regulator of endoplasmic reticulum stress and of the degradation of N-end rule and ubiquitin-fusion degradation pathway substrates in mammalian cells. *Mol. Biol. Cell.* **17:** 4606–4618.
34. Alzayady, K. J., M. M. Panning, G. G. Kelley, and R. J. Wojcikiewicz. 2005. Involvement of the p97-Ufd1-Npl4 complex in the regulated endoplasmic reticulum-associated degradation of inositol 1,4,5-trisphosphate receptors. *J. Biol. Chem.* **280:** 34530–34537.

35. Ron, D., and P. Walter. 2007. Signal integration in the endoplasmic reticulum unfolded protein response. *Nat. Rev. Mol. Cell Biol.* **8:** 519–529.
36. Ota, T., C. Gayet, and H. N. Ginsberg. 2008. Inhibition of apolipoprotein B100 secretion by lipid-induced hepatic endoplasmic reticulum stress in rodents. *J. Clin. Invest.* **118:** 316–332.
37. Su, Q., J. Tsai, E. Xu, W. Qiu, E. Bereczki, M. Santha, and K. Adeli. 2009. Apolipoprotein B100 acts as a molecular link between lipid-induced endoplasmic reticulum stress and hepatic insulin resistance. *Hepatology.* **50:** 77–84.
38. Sniderman, A. D., J. De Graaf, P. Couture, K. Williams, R. S. Kiss, and G. F. Watts. 2009. Regulation of plasma LDL: the apoB paradigm. *Clin. Sci. (Lond.).* **118:** 333–339.
39. Calderwood, S. K., A. Murshid, and T. Prince. 2009. The shock of aging: molecular chaperones and the heat shock response in longevity and aging–a mini-review. *Gerontology.* **55:** 550–558.